DOI: 10.1534/genetics.111.126797

Note

A Screenable *in vivo* Assay to Study Proteostasis Networks in *Caenorhabditis elegans*

Alexandra Segref, Serena Torres and Thorsten Hoppe[1]

Institute for Genetics and Cologne Excellence Cluster on Cellular Stress Responses in Aging-Associated Diseases, University of Cologne, 50674 Cologne, Germany

Manuscript received January 12, 2011
Accepted for publication January 31, 2011

ABSTRACT

In eukaryotic cells, the ubiquitin/proteasome system (UPS) is a key determinant of proteostasis as it regulates the turnover of damaged proteins. However, it is still unclear how the UPS integrates intrinsic and environmental challenges to promote organismal development and survival. Here, we set up an *in vivo* degradation assay to facilitate the genetic identification of ubiquitin-dependent proteolysis pathways in the multicellular organism *Caenorhabditis elegans*. Using this assay, we found that mild induction of protein-folding stress, which is nontoxic for wild-type worms, strongly reduces ubiquitin-dependent protein turnover. Ubiquitin-mediated degradation is also reduced by metabolic stress, which correlates with life-span extension. Unlike other stress conditions, however, acute heat stress results in enhanced rather than reduced proteolysis. Intriguingly, our study provides the first evidence for the existence of tissue-specific degradation requirements because loss of key regulators of the UPS, such as proteasomal subunits, causes accumulation of the model substrate, depending on the tissue type. Thus, here we establish a screenable degradation assay that allows diverse genetic screening approaches for the identification of novel cell-type-specific proteostasis networks important for developmental processes, stress response, and aging, thereby substantially extending the work on recently described mechanistic UPS reporter studies.

ENVIRONMENTAL conditions and developmental processes challenge the integrity of the proteome in every eukaryotic cell. The maintenance of proteostasis is a fundamental process orchestrated by refolding and degradation of unfolded proteins supporting organismal development and longevity (Powers *et al.* 2009). The ability to sustain protein quality control (PQC) is a long-term challenge for individual cells and entire organisms since high levels of damaged proteins accumulate during stress and aging. Defects in PQC affect proteostasis and often result in aggregation of unfolded proteins that can be toxic for cells. However, not all tissues are equally susceptible to the toxicity of protein aggregates (Gidalevitz *et al.* 2009), suggesting that there are tissue-specific differences in proteostasis pathways.

As part of the cellular PQC network, the ubiquitin/proteasome system (UPS) supports proteostasis by degradation of damaged proteins (Ciechanover *et al.* 2000; Kerscher *et al.* 2006). Substrates of the UPS are earmarked by covalent attachment of multiple ubiquitin molecules to an internal lysine residue. Typically, a chain of about four to six ubiquitin moieties is necessary and sufficient to target a substrate for degradation by the 26S proteasome, a multi-catalytic protease complex (Richly *et al.* 2005; Zhang *et al.* 2009). Polyubiquitylation of substrate proteins is usually mediated by an enzymatic cascade based on ubiquitin-activating enzymes (E1), ubiquitin-conjugating enzymes (E2), and ubiquitin protein ligases (E3). However, recently it was shown that in some cases polyubiquitylation requires the additional activity of a ubiquitin-chain elongation factor, called E4 enzyme (Hoppe 2005). In *Saccharomyces cerevisiae*, Ufd2p is the first E4 originally discovered in a genetic screen for mutants that are impaired in the turnover of ubiquitin fusion degradation (UFD) substrates (Johnson *et al.* 1995). Other so-called UFD proteins required for UFD substrate turnover in yeast are Ufd1p, Npl4p, and Cdc48p (CDC-48.1 and CDC-48.2

Supporting information is available online at http://www.genetics.org/cgi/content/full/genetics.111.126797/DC1.

[1]*Corresponding author:* Institute for Genetics and Cologne Excellence Cluster on Cellular Stress Responses in Aging-Associated Diseases (CECAD), University of Cologne, Zuelpicher Str. 47A, 50674 Cologne, Germany. E-mail: thorsten.hoppe@uni-koeln.de

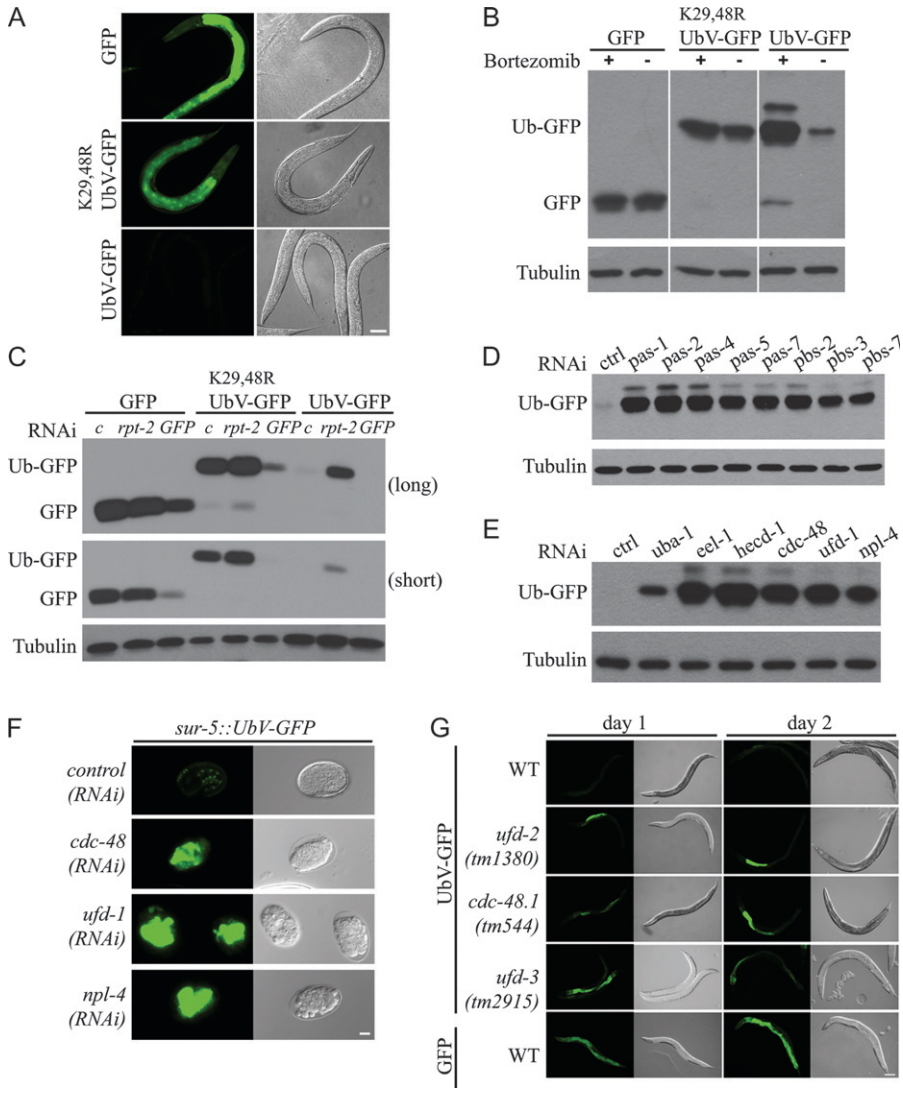

FIGURE 1.—*In vivo* detection of UPS activity. (A) Fluorescence and Nomarski images of L4-staged hermaphrodite worms expressing *GFP*, *UbV-GFP*, or ^{K29,48R}*UbV-GFP* from integrated transgenes under control of the *sur-5* promoter. Fluorescence images were taken with the same exposure time. Scale bar, 50 μm. (B) Protein extracts of the strains used in A that were treated with 10 nM bortezomib (+) or DMSO as control (−) were analyzed by immunoblotting with GFP antibodies. Tubulin was used as loading control. (C) Lysates of the strains used in A were RNAi-depleted for control (c, empty RNAi vector), *rpt-2*, or *GFP* and analyzed by immunoblotting as in B. Long and short exposure is shown for comparison. (D and E) Lysates of worms expressing *UbV-GFP* and lacking the indicated genes were analyzed as in B. (F) Embryos carrying the *sur-5::UbV-GFP* transgene and depleted for the indicated genes by RNAi were imaged with fluorescence and Nomarski optics as in A. Scale bar, 10 μm. (G) Fluorescence (same exposure) and Nomarski images of adult worms carrying the integrated transgenes *sur-5::UbV-GFP* (UbV-GFP) or *sur-5::GFP* (GFP) in N2 (WT, wild type) and the indicated deletion mutants at day 1 and day 2 of adulthood. Scale bar, 100 μm.

in *Caenorhabditis elegans*, p97 in mammals) (RICHLY *et al.* 2005). Together with the cofactors Ufd1p and Npl4p, Cdc48p forms a complex that functions as a ubiquitin-selective chaperone in substrate recruitment and ubiquitin chain assembly (RAPE *et al.* 2001).

Detailed mechanistic insights in UPS regulation have been obtained in extensive studies during the past decade. However, those studies in yeast and tissue culture experiments are limited in their approaches in gaining further insight into the physiological relevance of ubiquitin-dependent degradation during development and survival of multicellular organisms. Here, we established an *in vivo* degradation assay to study protein turnover during development and in differentiated tissues in response to intrinsic and environmental challenges. In contrast to already existing degradation assays in tissue culture, invertebrates, or mice, applicable to mechanistic studies but not to high-throughput screening approaches (JOHNSON *et al.* 1995; DANTUMA *et al.* 2000; LINDSTEN *et al.* 2003; HAMER *et al.* 2010), our *in vivo* degradation assay is suitable for the genetic identification of novel proteolysis factors and pathways important for developmental processes and longevity. Using this approach, we demonstrate cell-type-specific requirements for degradation factors of the UPS, which intriguingly suggest the existence of tissue-dependent proteostasis pathways rather than similar requirements in all tissues. Moreover, low doses of different stresses have an influence on the UPS, suggesting that different PQC pathways are activated through the existence of specialized stress sensors. In summary, we established an *in vivo* degradation assay that can serve to monitor and compare proteolytic networks, which are important in maintaining proteostasis during physiological and developmental challenges of whole organisms.

An *in vivo* degradation assay in *C. elegans*: To establish an *in vivo* degradation assay in a multicellular organism, we engineered a UFD model substrate in which a non-cleavable ubiquitin is N-terminally fused to GFP (UbV-GFP) and expressed under control of the *sur-5* promoter that is active in most tissues of *C. elegans* (GU *et al.* 1998). To rule out differences based on the expression of the

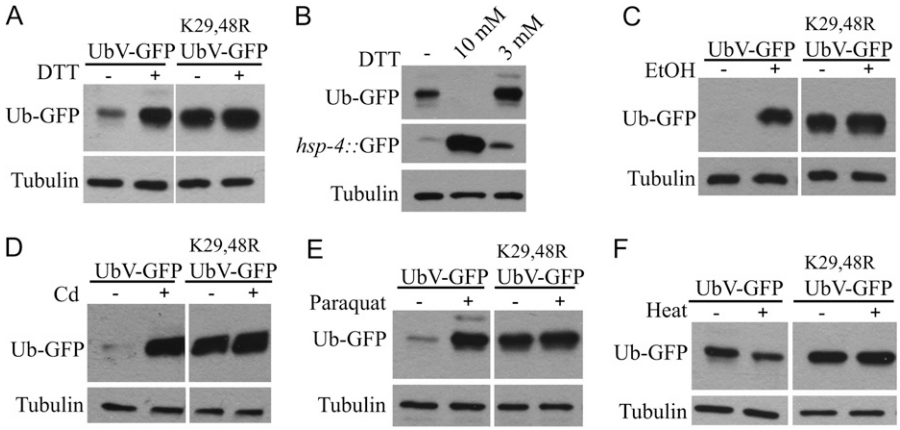

FIGURE 2.—Modulation of ubiquitin-dependent proteolysis by proteotoxic stress conditions. (A) Lysates of adult worms carrying *sur-5::UbV-GFP* treated with (+) or without (−) 3 mM DTT were analyzed by immunoblotting with GFP and tubulin antibodies. (B) Worms carrying *sur-5::UbV-GFP* or *hsp-4::GFP* were treated without (−) or with 10 mM or 3 mM DTT and analyzed as in A. (C) As in A, but worms were treated with or without 1% ethanol. (D) As A, but worms were treated with or without 100 μM cadmium. (E) As A, but worms were treated with or without 2 mM paraquat. (F) As A, but worms were grown to day 1 of adulthood and subjected to 37° for 2 hr (+) or as control (−) were kept at 20°.

transgene influencing the amount of substrate protein, *GFP* alone or *mCherry* were similarly expressed under control of the same promoter, and the constructs were stably integrated into the genome of *unc-119(ed4)* worms (MADURO and PILGRIM, 1995; PRAITIS *et al.* 2001). All strains used display comparable transgene expression as revealed by quantification of the mRNA levels (supporting information, Figure S1). Whereas GFP alone accumulates in several tissues including the hypodermis that surrounds the pharynx, the tail, vulva, and the intestine (GU *et al.* 1998), no fluorescent signal is detectable in worms carrying the *UbV-GFP* fusion construct (Figure 1A). However, replacement of lysine (K) residues 29 and 48 with arginine (K29, 48R) in the ubiquitin moiety results in stabilization of UbV-GFP, corroborating previous findings in budding yeast (JOHNSON *et al.* 1995). Given the lack of GFP signal in worms expressing UbV-GFP, ubiquitylation of the UFD substrate at K29 and K48 is likely to cause its proteasomal degradation. Indeed, incubation of transgenic worms with the proteasome inhibitor bortezomib specifically stabilizes UbV-GFP but does not affect the protein level of GFP or ^{K29,48R}UbV-GFP (Figure 1B). To confirm the importance of the 26S proteasome for degradation of the UFD substrate, we depleted individual proteasomal subunits by RNA interference (RNAi). Similar to bortezomib treatment, *rpt-2(RNAi)* or depletion of other proteasomal subunits stabilized UbV-GFP (Figure 1, C and D). The downregulation of GFP or ^{K29,48R}UbV-GFP by *GFP(RNAi)* shows that all tissues expressing *sur-5* can be efficiently targeted by RNAi treatment (Figure 1C and Figure 3A). Intriguingly, stabilization of UbV-GFP in animals lacking both p97 homologs CDC-48.1 and CDC-48.2 [hereafter referred to as CDC-48 depletion or *cdc-48.1/cdc-48.2(RNAi)*], UFD-1, NPL-4, UFD-2, or UFD-3 suggests the existence of a conserved UFD pathway in *C. elegans* (Figure 1E, E and G). To identify the corresponding E3 enzyme, we performed sequence comparison of the *C. elegans* genome to yeast Ufd4p and screened the potential candidates in our degradation assay. Interestingly, we found HECD-1 and EEL-1 to be important for degradation of the UFD substrate (Figure 1E). Thus, expression of the UPS model substrate UbV-GFP helped us to identify novel endogenous degradation factors in *C. elegans*.

Following the GFP signal during differentiation and development demonstrated that the UFD substrate accumulates in arrested embryos lacking CDC-48, UFD-1, or NPL-4, which is consistent with the fact that the CDC-$48^{UFD-1/NPL-4}$ complex is essential for cell cycle progression during embryogenesis (Figure 1F) (MOUYSSET *et al.* 2008). Thus, the UFD reporter substrate can be used to identify essential genes that regulate proteostasis during embryogenesis. The existence of null mutations of the UFD pathway that accumulate the substrate post-embryonically during adulthood suggests that defects in proteostasis are not necessarily lethal (Figure 1G). Therefore, forward genetic screens can identify mutants that abrogate proteolysis without affecting development.

UPS function is affected by protein-folding stress: Previous work in *S. cerevisiae* showed that certain mutants of the UPS are hypersensitive to elevated stress conditions, causing an accumulation of unfolded proteins in the cell (JUNGMANN *et al.* 1993; KERSCHER *et al.* 2006). To determine whether protein-folding stress influences ubiquitin-dependent protein degradation in animals with an unaffected UPS, we challenged wild-type worms expressing the UFD model substrate with different stressors. Intriguingly, worms treated with low levels of DTT (3 mM) specifically stabilized the UbV-GFP substrate expressed under the *sur-5* promoter (Figure 2, A and B). This low dose of DTT had only a mild effect on ER stress as shown by the use of the inducible *hsp-4::GFP* reporter that monitors ER stress (URANO *et al.* 2002). In contrast, treatment with a high dose of DTT (10 mM) caused a high level of ER stress and led to a lack of the UbV-GFP substrate, presumably by affecting its expression (Figure 2, A and B). Similarly, exposing worms to low doses of ethanol, the heavy metal cadmium, or the oxidative stress-inducing agent paraquat resulted in strong stabilization of UbV-GFP (Figure 2,

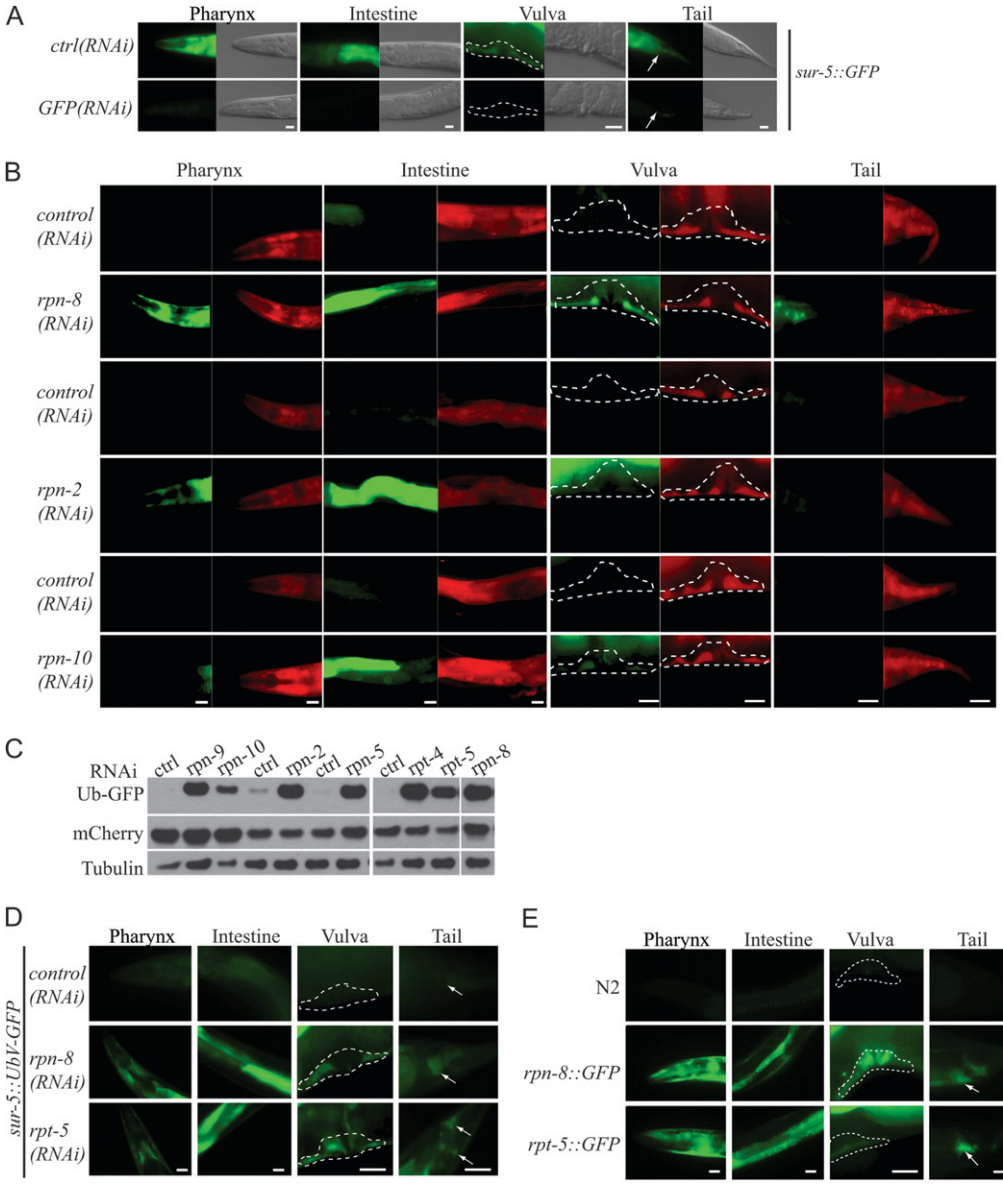

FIGURE 3.—Cell-type-specific requirements for degradation factors of the UPS. (A) Fluorescence and Nomarski images of worms expressing *sur-5::GFP* were grown on control plates [*ctrl(RNAi)*] or depleted for *GFP* by RNAi. Scale bars, 20 μm. Fluorescence images were taken with the same exposure time. (B) Hermaphrodites expressing *sur-5::UbV-GFP* and *sur-5::mCherry* were RNAi-depleted for *rpn-8*, *rpn-2*, or *rpn-10* as compared to the empty vector control and fluorescence images taken of GFP (green) and mCherry (red) at the same exposure times, respectively. Dashed outlines highlight the regions of interest. Scale bars, 20 μm. Note that the RNAi was applied for different time points (see Table S2), so for each RNAi experiment the corresponding control is depicted at the top. (C) Western blot of extracts from hermaphrodites containing the *sur-5::UbV-GFP* and *sur-5::mCherry* transgenes after control RNAi (ctrl, empty vector) or RNAi against the indicated proteasomal subunits. Because worms were analyzed at different time points (see Table S2), the corresponding controls are always depicted at the left. The blots were probed against GFP, mCherry, and Tubulin. (D) UbV-GFP is stabilized in worms that were RNAi-depleted for *rpn-8* or *rpt-5*. Hermaphrodite worms were imaged during early adulthood as in A. Scale bars, 20 μm. (E) GFP expression driven by *rpn-8* and *rpt-5* promoters. Hermaphrodite worms were imaged during early adulthood. Arrows and dashed outlines highlight the regions of interest. Scale bars, 20 μm.

C–E). In contrast, however, acute heat stress enhanced rather than reduced turnover of UbV-GFP (Figure 2F). Since this heat-induced degradation depends on K29 and K48 of the N-terminal ubiquitin moiety, it seems to require polyubiquitylation of the UFD substrate. These results indicate that the UPS differently integrates diverse protein-folding stress pathways in *C. elegans*. Moreover, the reporter assay is able to serve as a specific biomarker to monitor environmental stress conditions that influence proteostasis of multicellular organisms.

Tissue-specific protein degradation pathways: The 26S proteasome is composed of one proteolytically active 20S core particle attached to two 19S regulatory particles (RPs) that are important for unfolding and translocation of ubiquitylated substrates into the central 20S core (FINLEY 2009). In multicellular organisms, the proteolytic function of the 26S proteasome is expected to occur similarly in all tissues. However, whether the expression or composition of certain subunits varies in individual cell types is presently unknown. Having proven by GFP depletion that RNAi is similarly efficient in all *sur-5*-expressing tissues (Figure 1C and Figure 3A), we further addressed the importance of different proteasomal subunits for degradation of the UbV-GFP substrate in various tissues of the worm categorized into hypodermal cells surrounding the pharynx, the intestine, vulva, and tail. As shown before, UbV-GFP is stabilized in lysates of worms depleted for proteasomal

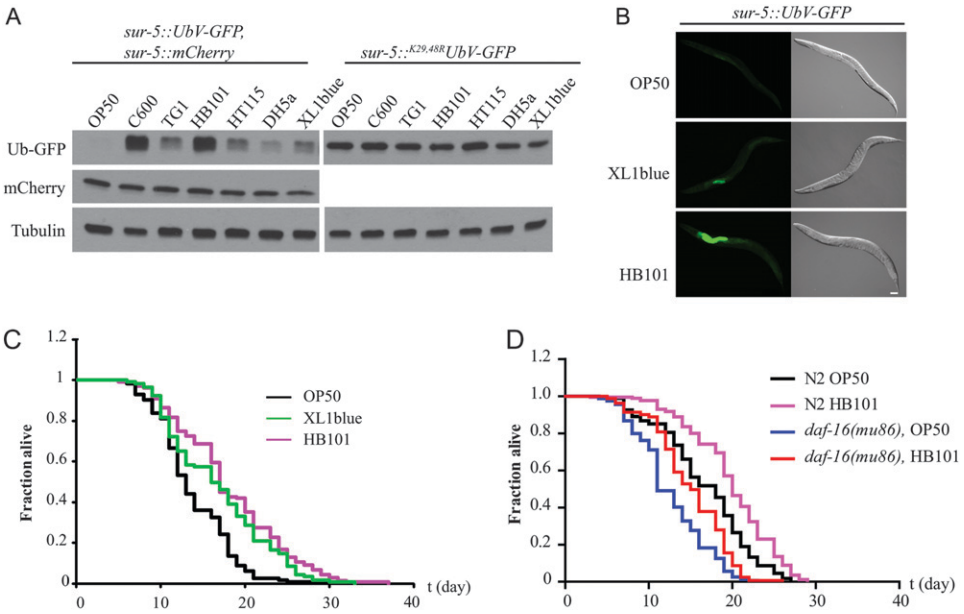

FIGURE 4.—The UFD reporter detects physiological changes. (A) Protein extracts of adult worms carrying the transgenes as indicated were fed with different *E. coli* strains and analyzed by immunoblotting with GFP, mCherry, or tubulin antibodies. (B) Fluorescence and Nomarski images of hermaphrodites grown on different *E. coli*. (C) Life-span analysis of N2 wild-type worms grown on plates containing the designated *E. coli* strains. (D) Life-span analysis of N2 wild-type or *daf-16(mu86)* mutant worms grown on plates containing the designated *E. coli* strains.

subunits (Figure 1, C and D). Given the essential role of the 20S subunits, their depletion resulted in lethality of the worms (data not shown), and these worms displayed only a weak GFP signal in the intestine, most likely due to reduced transcript levels of *UbV-GFP* (Figure S2 and Table S1). In contrast, knockdown of most subunits of the 19S RPs showed stabilization in different tissues (Figure 3, B, C, and D; Figure S2; Figure S3; Table S1). Surprisingly, some RP subunits support degradation of the UFD substrate in the hypodermis surrounding the pharynx and in the vulva, tail, and intestine (*i.e.*, *rpn-8*, *rpt-5*), whereas other subunits were not required in most tissues examined (*i.e.*, *rpn-10*) (Figure 3, B, C, and D; Figure S3B; Table S1). Since RNAi can efficiently downregulate *GFP* in the whole worm, it is unlikely that the tissue-specific differences in UFD substrate turnover between worms lacking the proteasomal subunits are due to incomplete RNAi depletion (Figure 1C and Figure 3A). To rule out that transcriptional or translational regulation contributes to changes in UFD substrate levels, we co-expressed both *UbV-GFP* and *mCherry* under the same promoter and compared the GFP and mCherry levels (Figure 3, B and C). In contrast to the UFD substrate, we did not detect any changes in mCherry amounts upon RNAi depletion of individual 19S subunits, indicating that the enhanced UbV-GFP levels are due to differential degradation rather than transcriptional changes. Thus, although the proteasome is required in all cell types, certain subunits of the 26S proteasome seem to be differently required or expressed in individual tissues of the worm.

In support of this idea, a comparison of the expression level of a subunit and its effect on protein stability revealed a strong correlation. For example, the tissue-specific stabilization of UbV-GFP upon RNAi depletion is related to the expression of the proteasomal subunits RPN-8 and RPT-5 (Figure 3, D and E; Table S3). Similarly, UFD pathway regulators required for ubiquitylation of the UFD substrate also demonstrate cell-type-specific activities (Figure 1G; Figure S3A; Table S1), which was confirmed by both RNAi treatment and loss-of-function mutants (Figure S3A; Table S1). These surprising observations suggest the existence of tissue-specific proteostasis networks and open completely new screening strategies. Genome-wide screening approaches based on fluorescent worm sorting will help to decipher proteolytic alterations between various tissues and how they are established during development.

Food source-dependent effects on proteolysis and longevity: Using different bacteria as a food source for the UPS reporter worms, we noted a direct influence of food on substrate turnover at day 1 of adulthood, which varied substantially with the *Escherichia coli* strains (Figure 4, A and B). In contrast to OP50 bacteria, XL1blue causes a modest and HB101 a strong stabilization of the UFD substrate preferentially in the intestine. Thus, depending on the food source, ubiquitin-dependent protein degradation is tissue-specifically perturbed in young adult worms. Recently, by using metastable proteins, the transition from larval development to adulthood was shown to be a critical time frame for the maintenance of proteostasis. Given that overexpression of the life-span-regulating transcription factor DAF-16 is able to override this critical event, a link between the regulation of proteostasis early in life and aging has been proposed (BEN-ZVI *et al.* 2009). Thus, we analyzed the influence of the different *E. coli* strains on life span in regard to the diverse effects on ubiquitin-dependent proteolysis. Interestingly, wild-type worms grown on HB101 showed an increased life span compared to OP50 bacteria, whereas XL1blue bacteria caused intermediate stabilization and life-span

extension. (Figure 4C, Table S4). The increased life span of HB101-fed worms is only partially suppressed by loss of *daf-16*, suggesting an alternative pathway that exists to link protein turnover with life span in the worm (Figure 4D, Table S5). Interestingly, the influence of nutrients on life-span extension was recently shown to depend on neuronal signaling (Maier *et al.* 2010). Altogether, these data suggest that metabolic changes are able to affect tissue-specific degradation pathways and longevity. It will thus be interesting to determine if neuronal signaling mutants that affect food source-dependent life-span regulation show defects in ubiquitin-dependent protein degradation.

In summary, our work reveals the existence of cell-type- and stress-specific degradation pathways required to differently integrate proteostasis networks throughout the development and aging of multicellular organisms. Our *in vivo* degradation assay provides a powerful tool for combining genetic screens based on sorting GFP fluorescence in worms and next-generation sequencing of the mutants discovered (Doitsidou *et al.* 2008; Sarin *et al.* 2008). This assay thereby offers unexplored avenues for the future investigation of key regulators and pathways central to cellular differentiation, stress response, and longevity. Similarly, it can serve as an economical approach for compound screens to design specific inhibitors of central UPS regulators. Furthermore, this screening assay can be easily adapted using alternative degradation signals to investigate additional proteolytic pathways such as the N-end rule pathway (Varshavsky 1992), ER-associated protein degradation (Meusser *et al.* 2005), or autophagy (Komatsu and Ichimura 2010).

We thank Y. Kohara, C. Riedel, the *Caenorhabditis* Genetics Center (funded by the National Institutes of Health National Center for Research Resources), the Dana-Farber Cancer Institute, and Geneservice for antibodies, plasmids, cDNAs, and strains. We are grateful for comments on the manuscript from M. Ermolaeva, A. Franz, W. Pokrzywa, U. Resch, and B. Schumacher. This work is supported by grants of the Deutsche Forschungsgemeinschaft (especially the Cologne Excellence Cluster on Cellular Stress Responses in Aging-Associated Diseases and the Research Unit FOR885) and the Rubicon European Union Network of Excellence (to T.H.). T.H. is a European Molecular Biology Organization Young Investigator.

LITERATURE CITED

Ben-Zvi, A., E. A. Miller and R. I. Morimoto, 2009 Collapse of proteostasis represents an early molecular event in Caenorhabditis elegans aging. Proc. Natl. Acad. Sci. USA **106:** 14914–14919.

Ciechanover, A., A. Orian and A. L. Schwartz, 2000 Ubiquitin-mediated proteolysis: biological regulation via destruction. Bioessays **22:** 442–451.

Dantuma, N. P., K. Lindsten, R. Glas, M. Jellne and M. G. Masucci, 2000 Short-lived green fluorescent proteins for quantifying ubiquitin/proteasome-dependent proteolysis in living cells. Nat. Biotechnol. **18:** 538–543.

Doitsidou, M., N. Flames, A. C. Lee, A. Boyanov and O. Hobert, 2008 Automated screening for mutants affecting dopaminergic-neuron specification in C. elegans. Nat. Methods **5:** 869–872.

Finley, D., 2009 Recognition and processing of ubiquitin-protein conjugates by the proteasome. Annu. Rev. Biochem. **78:** 477–513.

Gidalevitz, T., E. A. Kikis and R. I. Morimoto, 2009 A cellular perspective on conformational disease: the role of genetic background and proteostasis networks. Curr. Opin. Struct. Biol. **20:** 23–32.

Gu, T., S. Orita and M. Han, 1998 Caenorhabditis elegans SUR-5, a novel but conserved protein, negatively regulates LET-60 Ras activity during vulval induction. Mol. Cell. Biol. **18:** 4556–4564.

Hamer, G., O. Matilainen and C. I. Holmberg, 2010 A photoconvertible reporter of the ubiquitin-proteasome system in vivo. Nat. Methods **7:** 473–478.

Hoppe, T., 2005 Multiubiquitylation by E4 enzymes: 'one size' doesn't fit all. Trends Biochem. Sci. **30:** 183–187.

Johnson, E. S., P. C. Ma, I. M. Ota and A. Varshavsky, 1995 A proteolytic pathway that recognizes ubiquitin as a degradation signal. J. Biol. Chem. **270:** 17442–17456.

Jungmann, J., H. A. Reins, C. Schobert and S. Jentsch, 1993 Resistance to cadmium mediated by ubiquitin-dependent proteolysis. Nature **361:** 369–371.

Kerscher, O., R. Felberbaum and M. Hochstrasser, 2006 Modification of proteins by ubiquitin and ubiquitin-like proteins. Annu. Rev. Cell Dev. Biol. **22:** 159–180.

Komatsu, M., and Y. Ichimura, 2010 Selective autophagy regulates various cellular functions. Genes Cells **15:** 923–933.

Lindsten, K., V. Menendez-Benito, M. G. Masucci and N. P. Dantuma, 2003 A transgenic mouse model of the ubiquitin/proteasome system. Nat. Biotechnol. **21:** 897–902.

Maduro, M., and D. Pilgrim, 1995 Identification and cloning of *unc-119,* a gene expressed in the *Caenorhabditis elegans* nervous system. Genetics **141:** 997–988.

Maier, W., B. Adilov, M. Regenass and J. Alcedo, 2010 A neuromedin U receptor acts with the sensory system to modulate food type-dependent effects on C. elegans lifespan. PLoS Biol. **8:** e1000376.

Meusser, B., C. Hirsch, E. Jarosch and T. Sommer, 2005 ERAD: the long road to destruction. Nat. Cell Biol. **7:** 766–772.

Mouysset, J., A. Deichsel, S. Moser, C. Hoege, A. A. Hyman *et al.*, 2008 Cell cycle progression requires the CDC-48UFD-1/NPL-4 complex for efficient DNA replication. Proc. Natl. Acad. Sci. USA **105:** 12879–12884.

Powers, E. T., R. I. Morimoto, A. Dillin, J. W. Kelly and W. E. Balch, 2009 Biological and chemical approaches to diseases of proteostasis deficiency. Annu. Rev. Biochem. **78:** 959–991.

Praitis, V., E. Casey, D. Collar and J. Austin, 2001 Creation of low-copy integrated transgenic lines in *Caenorhabditis elegans.* Genetics **157:** 1217–1226.

Rape, M., T. Hoppe, I. Gorr, M. Kalocay, H. Richly *et al.*, 2001 Mobilization of processed, membrane-tethered SPT23 transcription factor by CDC48(UFD1/NPL-4), a ubiquitin-selective chaperone. Cell **107:** 667–677.

Richly, H., M. Rape, S. Braun, S. Rumpf, C. Hoege *et al.*, 2005 A series of ubiquitin binding factors connects CDC48/p97 to substrate multiubiquitylation and proteasomal targeting. Cell **120:** 73–84.

Sarin, S., S. Prabhu, M. M. O'Meara, I. Pe'er and O. Hobert, 2008 Caenorhabditis elegans mutant allele identification by whole-genome sequencing. Nat. Methods **5:** 865–867.

Urano, F., M. Calfon, T. Yoneda, C. Yun, M. Kiraly *et al.*, 2002 A survival pathway for Caenorhabditis elegans with a blocked unfolded protein response. J. Cell Biol. **158:** 639–646.

Varshavsky, A., 1992 The N-end rule. Cell **69:** 725–735.

Zhang, D., T. Chen, I. Ziv, R. Rosenzweig, Y. Matiuhin *et al.*, 2009 Together, Rpn10 and Dsk2 can serve as a polyubiquitin chain-length sensor. Mol. Cell **36:** 1018–1033.

Communicating editor: O. Hobert

GENETICS

Supporting Information
http://www.genetics.org/cgi/content/full/genetics.111.126797/DC1

A Screenable *in vivo* Assay to Study Proteostasis Networks in *Caenorhabditis elegans*

Alexandra Segref, Serena Torres and Thorsten Hoppe

DOI: 10.1534/genetics.111.126797

FILE S1

SUPPORTING MATERIALS AND METHODS

Strains

Worms were handled according to standard procedures and grown at 20°C unless otherwise stated (BRENNER 1974). Mutations and transgenes used in this study are listed by chromosomes as follows: *chn-1(by155)I, rpn-10(tm1349)I, cdc-48.1(tm544)II*, *ufd-2(tm1380)II, ufd-3(tm2915)II*, *unc-119(ed3)III*, *uba-1(it129)IV*. The Bristol strain N2 was used as wild-type strain.

Cloning procedures

Standard molecular biology protocols were used (SAMBROOK *et al.* 1989). *GFP*, *mCherry*, *UbV-GFP* and ^{K29,48R}*UbV-GFP* expression plasmids were constructed by PCR amplification of the corresponding cDNAs, the *sur-5* promoter region, the *unc-54* 3'UTR and cloned into pAS9. *rpn-5* and *pbs-1* genomic fragments were amplified by PCR and cloned into pPD129.36 for RNAi experiments.

RNAi

RNA interference was performed using the feeding method (MOUYSSET *et al.* 2008).

Generation of transgenic *C. elegans*

7 μg of linearized DNA constructs were bombarded into *unc-119(ed4)* mutants as described previously (PRAITIS *et al.* 2001).

RT-PCR

For semi-quantitative RT PCR 2 μg of total RNA isolated with the RNeasy kit (Qiagen) was used to perform the reverse transcriptase reaction with oligo(dT) primer using the Reverse Transcriptase kit (Invitrogen). For qRT-PCR 2.5 mg of total RNA was used to perform the reverse transcriptase reaction using the High capacity cDNA Reverse Transcription Kit (Applied Biosystems). The reaction was analyzed with the C1000 Thermal Cycler (Biorad) and the data processed with the Biorad CFX Manager 1.0.1 software.

In vivo imaging

Fluorescence images were taken with an Axio Imager.M1 microscope mounted with Axiocam MRm camera (Carl Zeiss) and processed with analysis software AxioVision 4.7 (Carl Zeiss). Pictures were processed with Adobe Photoshop CS4 for figure assembly.

Immunoblotting

Worms were lyzed in SDS sample buffer and equal volumes applied to SDS-PAGE. Western blotting was performed using antibodies against GFP (Clontech), mCherry (gift from C. Riedel) and Tubulin (Sigma).

Stress tests

L4 hermaphrodite worms were placed on NGM-plates containing 10 nM Bortezomib (Selleck Chemicals), 3 mM DTT, 2 mM paraquat (Sigma), 1% ethanol, or 100 μM cadmium (Sigma) (DMSO or H2O were added as control) and incubated for 12 hours. In heat shock experiments, day 1 adult worms were placed to 37°C or kept at 20°C for 2 hours.

Lifespan analysis

Lifespan assays were performed at 20°C; first day of adulthood was defined as day 0. From day 0 on, synchronized worm populations were transferred every 2-5 days to fresh NGM-medium plates. Worms were examined every day for touch-provoked movement and pharyngeal pumping, until death.

Statistics

Kaplan-Meier survival curves were generated using the WinSTAT for Excel 2007 and GraphPadPrism 5.03 software. The log-rank (Mantel–Cox) test was used to evaluate differences in survival and determine *P* values.

BRENNER, S., 1974 The genetics of Caenorhabditis elegans. Genetics **77:** 71-94.

MOUYSSET, J., A. DEICHSEL, S. MOSER, C. HOEGE, A. A. HYMAN *et al.*, 2008 Cell cycle progression requires the CDC-48UFD-1/NPL-4 complex for efficient DNA replication. Proc Natl Acad Sci U S A **105:** 12879-12884.

PRAITIS, V., E. CASEY, D. COLLAR and J. AUSTIN, 2001 Creation of low-copy integrated transgenic lines in Caenorhabditis elegans. Genetics **157:** 1217-1226.

SAMBROOK, J., E. F. FRITSCH and T. MANIATIS, 1989 *Molecular Cloning: A Laboratory Manual*. Cold Spring Habor Laboratory Press, Cold Spring Habor, NY.

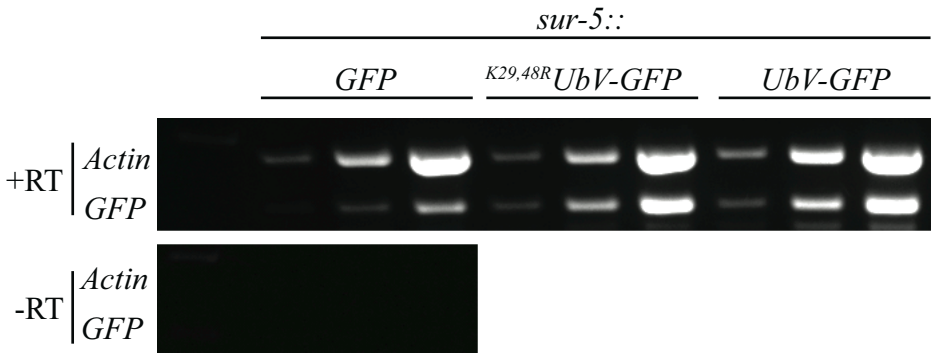

FIGURE S1.—mRNA expression levels of worms carrying the integrated transgenes under the control of the *sur-5* promoter. Semi-quantitative reverse transcriptase PCR was performed against *Actin* and *GFP* for 16, 18 and 20 PCR cycles in the presence (+ RT) or as a negative control in the absence (-RT) of reverse transcriptase. For − RT only 20 PCR cycles were performed.

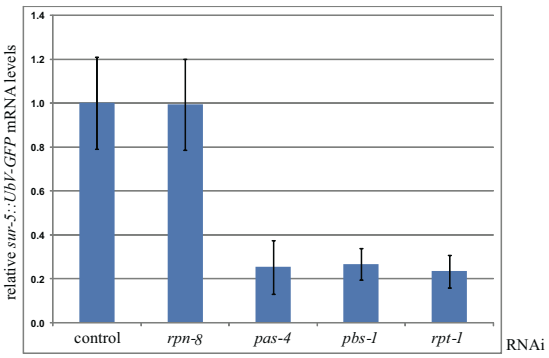

FIGURE S2.—Quantification of mRNA levels of *sur-5::UbV-GFP* by qRT-PCR after worms were treated with RNAi against different proteasome subunits. Relative expression compared to *lamin* mRNA is depicted.

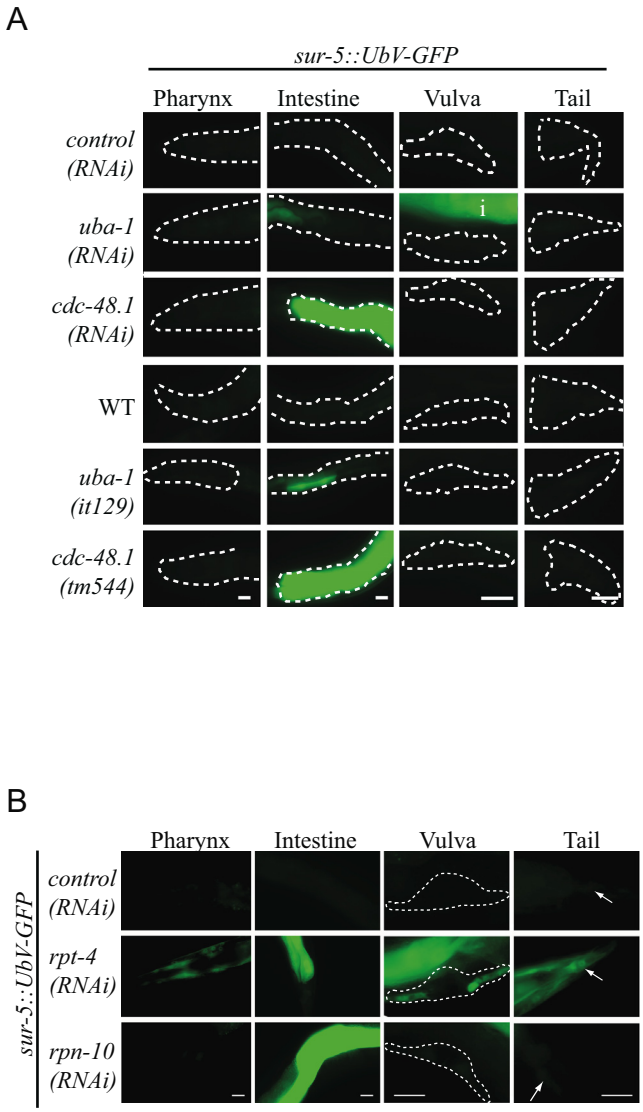

FIGURE S3.—A) Comparison of UbV-GFP stabilization between RNAi-treated worms and the corresponding deletion mutants, scale bars: 20 μm; part of the intestine (denoted as i) of *uba-1(RNAi)* worms. Circles highlight the regions of interest. (B) UbV-GFP is stabilized in worms that were RNAi depleted for *rpt-4 or rpn-10*. Hermaphrodite worms were imaged during early adulthood as in Fig. 3A.

TABLE S1

Stabilization of UbV-GFP in adult worms under control of the *sur-5* promoter after RNAi treatment or in mutant strains

Gene	Pharynx	Intestine	Vulva	Tail
pas-6 (RNAi)	+	+	+	+
*rpt-3 (RNAi)^*	+	+	+	+
*rpt-4 (RNAi)^*	+	+	+	+
rpn-3 (RNAi)#	+	+	+/-	+
rpn-6 (RNAi) #	+	+/-	+	+
rpn-7 (RNAi) #	+	+	+	+/-
rpn-8 (RNAi) #	+	+	+	+
rpn-11 (RNAi) #	+	+	+	+
*rpt-2 (RNAi)^*	+	+	+/-	+
*rpt-5 (RNAi)^*	+	+	+	+/-
*rpt-6 (RNAi)^*	+	+	+	+
cdc-48.1/2 (RNAi)	+	+	+	+
hecd-1 (RNAi)	+	+	+	+
rpn-1 (RNAi) #	+/-	+	-	-
rpn-2 (RNAi) #	+/-	+	-	-
rpn-5 (RNAi) #	+	+	-	+
rpn-9 (RNAi) #	+/-	+	+/-	-
rpn-10 (RNAi) #	-	+	+	-
npl-4 (RNAi)	+ /-	+	-	-
ufd-2(tm1380)	-	+	+/-	-
eel-1 (RNAi)	-	+	-	-
ufd-3 (RNAi)	-	+	-	-
ufd-3(tm2915)	-	+	-	-
let-70 (RNAi)	-	+	-	-
pas-1(RNAi)*	-	+	-	-
*rpt-1 (RNAi)^*	-	+	-	-
rpn-12 (RNAi) #	-	+/-	-	-
p27 (RNAi)	-	+/-	-	-
chn-1(RNAi)	-	+	-	-
chn-1(by155)	-	+	-	-
ufd-1 (RNAi)	-	+	-	-
uba-1 (RNAi)	-	+	-	-
uba-1(it129)	-	+	-	-

cdc-48.1(RNAi)	-	+	-	-
cdc-48.1(tm544)	-	+	-	-
cdc-48.2 (RNAi)	-	+	-	-
rpn-10 (tm1349) #	-	+	-	-

*All other 20S subunits (*pas-1-5,7* and *pbs1-7*) of the proteasome showed stabilization only in the intestine. # non-ATPase subunits of the 19S proteasome complex, ^ ATPase subunits of the 19S proteasome complex. Shading: grey: stabilization in all tissues, blue: stabilization in various tissues, white: stabilization in intestine.

TABLE S2

RNAi conditions used in the main paper

Gene	RNAi condition (stage applied, incubation time)
pas-1	L3, 48hr
pas-2	L3, 48hr
pas-3	L1, 48hr
pas-4	L3, 48hr
pas-5	L3,48hr
pas-6	L1, 48hr
pas-7	L3, 48hr
pbs-1	L3, 48hr
pbs-2	L3, 48hr
pbs-3	L3, 48hr
pbs-4	L3, 48hr
pbs-5	L3, 48hr
pbs-6	L3, 48hr
pbs-7	L3, 48hr
rpt-1	L3, 48 hr
rpt-2	L1, 48 hr
rpt-3	L1, 48hr
rpt-4	L1, 48hr
rpt-5	L1, 48hr
rpt-6	L3, 48hr
rpn-1	L3, 48hr
rpn-2	L3, 24hr, 48hr
rpn-3	L1, 48hr
rpn-5	L1, 48 hr
rpn-6	L1, 48hr
rpn-7	L1, 48hr
rpn-8	L3, 24hr, L1, 48hr
rpn-9	L1, 72hr
rpn-10	L1, 72hr
rpn-11	L1, 48hr
rpn-12	L1, 72hr
p27	L1, 72hr
hecd-1	L1, 48hr and 120hr
eel-1	L3, 48hr
chn-1	L1, 48hr

cdc-48/1.2	L1, 48hr, (L3, 72hr for embryos)
ufd-1	L1, 48hr, (L3, 72hr for embryos)
npl-4	L1, 120 hr, (L3, 72hr for embryos)
uba-1	L1, 48hr
ufd-3	L3, 48hr

Initially various conditions were tested for all genes and the condition where maximum stabilization of the *sur-5::*UbV-GFP was recorded (as indicated in this table) was chosen for further experiments.

TABLE S3

Comparison of promoter expression and protein stabilization after RNAi

Promoter/	Promoter expression				*sur-5::*UbV-GFP Stabilization			
RNAi	Pharynx	Intestine	Vulva	Tail	Pharynx	Intestine	Vulva	Tail
rpt-3	+	+/-	+	+	+	+	+	+
rpt-5	+	+	+/-	+	+	+	+	+/-
rpn-2	-	+	-	-	+/-	+	-	-
rpn-5	+	+	+	+	+	+	-	+
rpn-8	+	+	+	+	+	+	+	+

Green shading: correlation of promoter expression and UbV-GFP stabilization.

TABLE S4

Statistical analysis of N2 Bristol grown on different *E. coli* from 3 experiments

Experiment 1	Mean lifespan/d	Stdv	n	p value (t-test)	p-value (Mantel-Cox)
OP50	13.14	4.3	35		
XL1blue	16.34	4.8	35	0.0045	0.0031
HB101	17.56	6.9	45	0.0014	0.0003
XL1blue/HB101				0.0073	0.0018
Experiment 2					
OP50	13.76	4.6	41		
XL1blue	17.67	6.1	42	0.0014	0.0019
HB101	19.08	6.6	48	< 0.0001	< 0.0001
XL1blue/HB101				0.2811	0.3233
Experiment 3					
OP50	14.57	4.3	35		
XL1blue	15.97	7.0	38	0.3115	0.1151
HB101	17.37	5.9	38	0.0240	0.0117
XL1blue/HB101				0.0032	0.0056
All combined					
OP50	13.82	4.4	111		
XL1blue	16.70	6.0	115	< 0.0001	< 0.0001
HB101	18.06	6.5	131	< 0.0001	< 0.0001
XL1blue/HB101				0.0002	< 0.0001

n: number of animals analyzed

TABLE S5

Statistics for lifespan experiments of WT or *daf-16(mu86)* worms grown on different *E.coli*

Experiment 1	Mean lifespan/d	Stdv	n	P -value (t-test)		P-value (Mantel-Cox)
N2 OP50	15.98	5.2	46			
N2 HB101	19.10	5.1	45	N2 OP50	< 0.0001	0.0043
daf-16(mu86)	12.30	4.3	43	N2 OP50	< 0.0001	0.0002
OP50				N2 HB 101	< 0.0001	< 0.0001
daf-16 (mu86)	14.50	5.4	41	N2 HB101	< 0.0001	< 0.0001
HB101				*daf -16(mu86)* OP50	< 0.0001	0.0215
				N2 OP50	0.0088	0.1495
Experiment 2						
N2 OP50	16.0	5.3	44			
N2 HB101	19.80	5.4	39	N2 OP50	< 0.0001	0.0008
daf-16(mu86)	12.0	4.0	40	N2 OP50	< 0.0001	< 0.0001
OP50				N2 HB101	< 0.0001	< 0.0001
daf-16 (mu86)	15.0	3.5	42	N2 HB101	< 0.0001	< 0.0001
HB101				*daf -16(mu86)* OP50	< 0.0001	0.0053
				N2 OP50	0.0682	0.0223
Experiment 3						
N2 OP50	17.50	5.2	44			
N2 HB101	20.10	5.0	44	N2 OP50	< 0.0001	0.0286
daf-16(mu86)	13.20	4.0	37	N2 OP50	< 0.0001	< 0.0001
OP50				N2 HB101	< 0.0001	< 0.0001
daf-16 (mu86)	16.40	3.8	41	N2 HB101	< 0.0001	< 0.0001
HB101				*daf -16(mu86)* OP50	< 0.0001	0.0015
				N2 OP50	0.0515	0.0372
Experiment 4						
N2 OP50	17.50	6.0	44			
N2 HB101	21.0	4.3	42	N2 OP50	< 0.0001	0.0161
daf-16(mu86)	13.10	4.7	39	N2 OP50	< 0.0001	0.0001
OP50				N2 HB101	< 0.0001	0.0001
daf-16 (mu86)	14.20	4.2	37	N2 HB101	< 0.0001	0.0001
HB101				*daf -16(mu86)* OP50	< 0.0001	0.387
				N2 OP50	< 0.0001	0.0004
All combined						
N2 OP50	16.73	5.4	175			
N2 HB101	19.95	4.9	170	N2 OP50	< 0.0001	< 0.0001
daf-16(mu86)	12.64	4.2	159	N2 OP50	< 0.0001	< 0.0001

OP50				N2 HB101	< 0.0001	< 0.0001
daf-16 (mu86)	15.03	4.3	161	N2 HB101	< 0.0001	< 0.0001
HB101				*daf-16(mu86)* OP50	< 0.0001	< 0.0001
				N2 OP50	0.0106	< 0.0001

n: number of animals analyzed.